Renewable and Sustainable Energy Reviews 34 (2014) 8–19

Contents lists available at ScienceDirect

Renewable and Sustainable Energy Reviews

journal homepage: www.elsevier.com/locate/rser

Exergoeconomic analysis of high concentration photovoltaic thermal co-generation system for space cooling

Veronica Garcia-Heller, Stephan Paredes, Chin Lee Ong, Patrick Ruch, Bruno Michel *

Advanced Micro Integration, IBM Research Zurich, Säumerstrasse 4, 8803 Rüschlikon, Switzerland

ARTICLE INFO

Article history:
Received 18 September 2013
Received in revised form
29 January 2014
Accepted 18 February 2014
Available online 19 March 2014

Keywords:
Photovoltaics
Exergy
NPV
Thermal
Co-generation
Tri-generation

ABSTRACT

This paper provides an exergetic analysis of a 10 MW high concentration photovoltaic thermal (HCPVT) power plant case study located in Hammam Bou Hadjar, Algeria. The novel HCPVT multi-energy carrier plant converts 25% of the direct normal irradiance (*DNI*) into electrical energy and 62.5% to low grade heat for a combined efficiency of 87.5%. The HCPVT system employs a point focus dish concentrator with a cooled PV receiver module. The novel "hot-water" cooling approach is used for energy reuse purposes and is enabled by our state-of-the-art substrate integrated micro-cooling technology. The high performance cooler of the receiver with a thermal resistance of $<0.12\ cm^2\ K/W$ enables the receiver module to handle concentrations of up to 5000 suns. In the present study, a concentration of 2000 suns allows using coolant fluid temperatures of up to 80 °C. This key innovation ensures reliable operation of the triple junction PV (3JPV) cells used and also allows heat recovery for utilization in other thermal applications such as space cooling, heating, and desalination. Within this context, an exergoeconomics analysis of photovoltaic thermal co-generation for space cooling is presented in this manuscript.

The valuation method presented here for the HCPVT multi-energy carrier plant comprises both the technical and economic perspectives. The proposed model determines how the cost structure is evolving in four different scenarios by quantifying the potential thermal energy demand in Hammam Bou Hadjar. The model pins down the influence of technical details such as the exergetic efficiency to the economic value of the otherwise wasted heat. The thermal energy reuse boosts the power station's overall yield, reduces total average costs and optimizes power supply as fixed capital is deployed more efficiently. It is observed that even though potential cooling demand can be substantial (19,490 MWh per household), prices for cooling should be 3 times lower than those of electricity in Algeria (18 USD/MWh) to be competitive. This implies a need to reach economies of scale in the production of individual key components of the HCPVT system. The net present value (*NPV*) is calculated taking growth rates and the system's modular efficiencies into account, discounted over 25 years. Scenario 1 shows that even though Algeria currently has no market for thermal energy, a break-even quantity (49,728 MWh) can be deduced by taking into account the relation between fixed costs and the marginal profit. Scenario 2 focuses on the national growth rate needed to break even, i.e. +10.92%. Scenario 3 illustrates thermal price variations given an increase in the Coefficient of Performance (COP) of a thermally driven adsorption chiller after year 10. In this case, the price for cooling will decrease from 18 USD/MWh to 14 USD/MWh. Finally, scenario 4 depicts Hammam Bou Hadjar's potential cooling demand per household and the growth rate needed to break even if a market for heat would exist.

Contents

* Corresponding author. Tel.: +41 44 724 86 48.
E-mail address: bmi@zurich.ibm.com (B. Michel).

http://dx.doi.org/10.1016/j.rser.2014.02.037
1364-0321/

1. Introduction

The economics of solar energy have been changing in the recent years in terms of cost, champion technology and locations. Photovoltaic (PV) deployments in subsidized markets grew beyond expectation in the last five years. During 2011, Italy and Germany provided about 57% of new PV operating capacity for the European Union [1]. However, reduced incentives and dramatic module cost reduction cause a shift of primary markets to more sunny locations. In addition, reduced module cost makes balance of system (BOS) cost more important which places a higher value on efficiency. This is advantageous for concentrated photovoltaic (CPV) systems with a module efficiency exceeding 30%. More concretely, advantages of CPV are a lower capital investment [2] and a steeper learning curve because of the reduced usage of semiconductor material. CPV systems show a higher energy yield per module and a lower levelized cost of energy (LCOE) because their active tracking system improves the match between output and load profile.

Several studies evaluated the economic feasibility of PV plants [3–5] through the LCOE metric. The latter is calculated using a mix of independent variables. Some of those variables have a direct impact in the LCOE, affecting the final results. To understand how each individual variable impacts the final LCOE a sensitivity analysis is usually performed. Those studies also identify the advantage PV has over CSP when it comes to capturing diffuse and direct solar irradiation [6]. While the technology with the largest deployment in hot climates has been concentrated solar power (CSP) [3] with trough collectors, thermal storage, and steam engines, this technology is coming more and more under pressure [7]. Despite the recent large progress in efficiency, photovoltaic as well as solar thermal installations can only make use of a minor fraction of the incident radiation, typically less than 30%. This motivates the design of solar systems that combine the production of electrical energy with usable heat, i.e. for cooling applications to achieve total (exergy compensated) yields beyond 30%.

Concentrating solar radiation onto the surface of a solar cell has been used since the 70s [8–10] and photovoltaic thermal (PVT) technologies with active cooling and heat use have been developed in parallel because of large thermal loads on PV cells [11–15]. Concentrated Photovolatic Thermal (CPVT) systems started spreading when analytical work showed how PV becomes more efficient and cheaper with concentrated irradiance [16]. This required the development of optics and tracking systems [17,18] and combinations between solar systems, heat pumps, and heat use [19]. The key metric combined electrical and thermal efficiency started rising reaching values of 69% [20] which eventually opened the path to concentrating photovoltaic thermal plants [21,22]. The need for investment into high performance cooling solutions and low resistance electrical packaging became apparent with the inverse relationship between the temperature in the solar cell and the electrical and the effect of series resistance [23]. Several overviews describing all details for concentrating PV systems are available in recent literature [24–28] and summaries on more recent efforts on standardization of actively cooled CPV and CPVT systems are available as well [29].

Exergy is the best quantity to outline the capability of the system to generate a thermal and an electrical output in an efficient manner. Exergy reveals the available useful energy necessary for energy planning and the commercialization of a power plant. In fact, commercial and residential consumers demand energy services offered by different power providers. Co-generation and tri-generation plants are characterized by complex interactions between the generation, storage, conversion and the transportation system. These power plants are able to produce electricity, heating and/or cooling from a particular energy source. Co-generation and tri-generation plants enable energy savings while being environmentally friendly [30]. To improve energy savings in cogeneration systems a bigger yield should be achieved from the process and consequently reducing the consumption of the natural resource [31]. A number of studies addressed the proportion of solar radiation converted into electricity and heat [32–34]. The exergy analysis of the PV module and thermal energy carriers such as air and water are proposed in Refs. [35–39], while a more detailed economic analysis was conducted in Refs. [40–46].

The main reason for the changes in the field of solar energy and increased attractiveness of co-generation technologies is attributed to the growing demand for cooling and desalination. The International Energy Agency (IEA) predicts nearly a tripling of worldwide cooling demand, with even higher growth in emerging economies in the Sunbelt [47] in the timeframe from 2010 to 2050. In these economies, demand for cooling can only be satisfied almost completely with compression chillers. Increased consumption will strain electrical grids and power stations, which in turn opens new opportunities for energy transport. In recent years, more efficient thermally driven sorption cooling methods have been developed, i.e. absorption and adsorption cooling. Absorption cooling relies on sorption of a working fluid in another fluid while adsorption cooling works with desorption and adsorption of a working fluid from a porous solid. While the optimal driving temperature for absorption cooling needs lies above 90 °C, adsorption cooling can operate efficiently with driving temperatures below 90 °C [48]. On the other hand, the demand for desalination in water scarce regions is growing even faster than the demand for cooling. High population growth in these arid regions, changes in rainfall patterns, waterway pollutions and depletion of “fossil water” in aquifers are driving the human population to seek alternative renewable water resources, i.e. desalination. Traditionally, desalination can be carried out with mechanically driven membrane separation processes like reverse osmosis (RO) and thermally driven methods such as multi-stage flashing (MSF), multi-effect boiling (MEB) and membrane distillation (MD). Comparing the thermally driven desalting methods, conventional MSF and MEB rely on high driving temperatures, typically higher than 100 °C, while MD requires driving temperatures of 70–90 °C, which is comparable to newer generations of low temperature distillation systems (LT-MED). In general, the medium grade heat requirement of adsorption cooling and membrane distillation enables new approaches for solar multi-generation making them the perfect candidates as potential thermal users of the HCPVT system [49].

The challenge of such a co-generation system is to fairly assess the relative economic value of the electrical and thermal output in view that a multi-objective-optimization process can be applied. An important challenge is the transport system to the user, since electrical and thermal transport have very different investment cost, maintenance cost and distance dependent losses. One of the advantages of the HCPVT solar farm resides in the transportation

Nomenclature

A	area of living space [m^2]
A_l	total solar collector area [m²]
A_{pipe}	pipe cross section area [m²]
CDH	cooling degree hours [–]
COP_{el}	Electrical Coefficient of Performance [–]
COP_{th}	Thermal Coefficient of Performance [–]
c_p	specific heat [J/kg K]
D	total demand [USD]
D_{t+1}	quantity demand per period [–]
D_{pipe}	pipe diameter [m]
D_{th}	thermal demand [–]
DNI_{nom}	nominal direct normal irradiance [W/m²]
DNI_{max}	maximal direct normal irradiance [W/m²]
E_t	expenditures per period [USD]
E_{th}	thermal capacity [MWh]
$f_{fanning}$	fanning's friction factor [–]
i	interest rate [%]
K	insulation [–]
L	length [m]
$\dot{m}$	mass flow rate [kg/s]
N	number of people per household [–]
NPV	net present value [USD]
P	benchmark price [USD]
P_{el}	Algeria's electricity price [USD]
P_{th}	price of thermal energy [USD]
$\dot{Q}$	heat flow [W]
Q_{pump}	pumping energy [kWh]
$\dot{Q}_{th}$	thermal power [W]
$\dot{Q}_{gen}$	generated thermal power [MW]
R_t	receipts [USD]
Re	Reynold's Number [–]
T_i	hourly temperature [°C]
T_{ref}	reference temperature [°C]
t	period [yr]
t_{max}	maximum sun hours [h]
t_{peak}	peak sun hours [h]
$\dot{V}$	volumetric flow rate [m3/s]
ν	mean velocity [m/s]

Greek letters

Ψ	overall system efficiency [%]
γ	variable costs [USD]
β	fixed costs [USD]
$\eta_{th,1}$	system thermal efficiency [%]
$\eta_{th,2}$	adsorption chiller's coefficient of performance [–]
η_{el}	electrical efficiency [%]
η_{th+el}	overall efficiency of the system [%]
$\eta_{concentrator}$	efficiency of the concentrator (tracking and primary optics) [%]
$\eta_{receiver}$	efficiency of the receiver [%]
$\eta_{inverter}$	efficiency of the inverter [%]
$\eta_{s\ optics}$	efficiency of the secondary optics [%]
$\eta_{th,\ coll}$	thermal collection efficiency
φ	specific dwelling characteristics [–]
ε	elasticity [–]
π	profit [USD]
Δp	pressure drop [bar]
ΔT	temperature gradient [K]
μ	dynamic viscosity [Pa s]
ρ	density [kg/m^3]

system since it diversifies the way energy is usually transported, i.e. through the electrical grid. Therefore, in regions with high space cooling demand, congestion issues become less severe in the power grid. For thermal transport systems no such congestion is created since cooling energy can be stored orders of magnitude cheaper than electrical energy.

The prime objective of this manuscript is to determine whether solar energy can be utilized efficiently in trigeneration for space cooling and heating applications and to determine the value of heat in Hammam Bou Hadjar, a region with high solar irradiance and cooling demand. Naturally, electrical energy (a high grade energy source) which can easily be converted into other energy forms is more expensive when compared to low grade thermal energy. Moreover, thermal energy prices are typically not set by any power plant operator which makes it challenging to determine prices. In addition, space cooling is growing quickly among emerging economies [50]. Therefore, load behavior is estimated for cooling and heating activities per unit of time for a residential surface in Algeria. This allows a better system design for an underlying consumption pattern. In this paper, we describe thermal demand for cooling application and match it with the HPCVT capacity given its technological constraints. Among those, transmission services are taken into account because they reflect the physical limitations to ensure system operation, stability and control.

2. Methodology

From a technological perspective, the value of heat can be illustrated as a tradeoff between the transportation losses and the global thermal output. In the model, we have implemented a system design that estimates (i) the land area needed by solar collectors, (ii) storage requirements, (iii) pumping power, and finally (iv) the total output (electrical and thermal). In addition, a well-executed design allows approximation of the total capital needed to service demand. The average thermal cycles are captured using cooling/heating degree days and hours coupled with specific living space features. Hence, a simulation was carried out with the Polysun software package [51] to capture the potential thermal energy demand per household in Hammam Bou Hadjar. Polysun is an efficient and state of the art simulation tool for different energy systems [52] which enables the quantification of the household thermal energy demand. We merge the technical and economic approach using weather data from Meteonorm [53] to observe demand patterns among residential users in Hammam Bou Hadjar at a specific point in time. It is observed that Hammam Bou Hadjar has a high potential demand for cooling.

In fact, beyond the learning curve approach [54] a more detailed growth pattern is applied. Growth rates are considered in the calculation of the *NPV* to illustrate the impact of economic and technological conditions over time. Other valuation methods highlighted in [55] were used to find the optimal design of a multi-energy carrier generating station. However, this paper does not use a real option valuation to highlight the uncertainty of energy prices in the future. Instead, this manuscript bases its formulation on the integration of two different outputs within a single generating station, a nodal piping structure and valuing the investment through the *NPV*, assuming a 25 year horizon in Hammam Bou Hadjar, Algeria. Similar co-generation projects [56] are being launched by the European Union. Such smart energy solutions aim to reduce carbon footprints, shift the electrical to thermal consumption, and reduce the electricity

bill per household. The success of multi-generating solutions (combined heat and power) in other areas implies that they also can be successful in sunny regions.

3. The technology

Hot water cooling, enabled by microchannel coolers allows high concentration photovoltaic thermal system to provide electrical energy, desalinated water, adsorption cooling and space heating making the system cost competitive [57,58]. The HCPVT system combines PV and solar thermal techniques: A hot-water-cooled multichip receiver mounted in the focal point of a parabolic concentrator generates both heat and electricity. Photovoltaic thermal concentrators (Fig. 1) generate electrical energy with an efficiency of $>25\%$, and simultaneously $\sim 50\%$ of reusable heat, for heating, water desalination, or adsorption cooling. The overall efficiency of such systems is, therefore, higher than 75%. The use of 2000-fold concentrated solar radiation reduces the amount of 3JPV cells but causes a power density above 150 W/cm². This power density parallels that of high-performance processors, so that similar advanced cooling solutions are needed. The use of active water cooling enables larger receivers and higher solar concentrations, which means lower energy costs and a higher electrical efficiency.

The deployment of HCPVT systems enables the conversion of solar energy to electricity and heat in regions with a *DNI* above 1800 kWh/m² yr. A study conducted by the German Aerospace Center pointed out that compared to its Mediterranean peers, Algeria's surface and insolation provides a much larger potential for solar energy [59]. In fact Hammam Bou Hadjar has a *DNI* of 2106 kWh/m²/yr. In addition to its favorable insolation and area, Algeria offers many other advantages whereby (i) the country is opening up its doors slowly to foreign investments, thus allowing a less restrictive investment policy in the near future for foreign companies, (ii) an attempt to gauge stability to its banking system by setting up a new rating organism, which is a hint for a change in Algeria's economic environment and (iii) electricity market deregulation as reported in [60]. Recent renewable energy projects organized by NEAL [61] and Solarpaces [62] promise new options for future PV developments in the Algerian region. A more competitive environment in the electricity market is often subjected to a better understanding and prediction of loads. Therefore, forecasting is not only required to optimize energy supply but also to comply with the rules set by the grid operator. However, given the stochastic nature of weather conditions, it is difficult to make a reliable prediction of solar power production for 7 days ahead. Still, technological growth propelled by innovative techniques, such as HCPVT farms, presents the advantage of having thermal storage capacity in place. This improvement enables flexibility of power supply when weather conditions do not allow a minimum level of production to satisfy the thermal load.

HCPVT is a technology that can be used for cogeneration of electrical and medium grade thermal output. The HCPVT system consists of four different building blocks: a primary point focus rotational symmetric parabolic concentrator mirror, a tracking system, the receiver module with an active cooling loop and a thermal storage system. The output of the system depends on the *DNI* and the sun tracking accuracy. Unlike most CPV systems, HCPVT allows concentrations beyond 1000 suns, allowing the efficient use of 87.5% of the collected solar radiation. Secondary optics must be applied to achieve a better distribution of the sun light to homogenize the illumination across photovoltaic cells [63]. Multi junction cells are preferred because their electrical conversion efficiency levels are high, e.g. up to 44% [64,65] for high concentrated light. Therefore, the combination of such cells with a high-performance cooling process can enable high system efficiencies at high concentrations. Thus, the improvement of the system efficiency and the ability of the cell to operate at higher concentrations imply an increase of the power output per receiver and a reduction in the number of receiver modules needed to obtain a predefined power output [66].

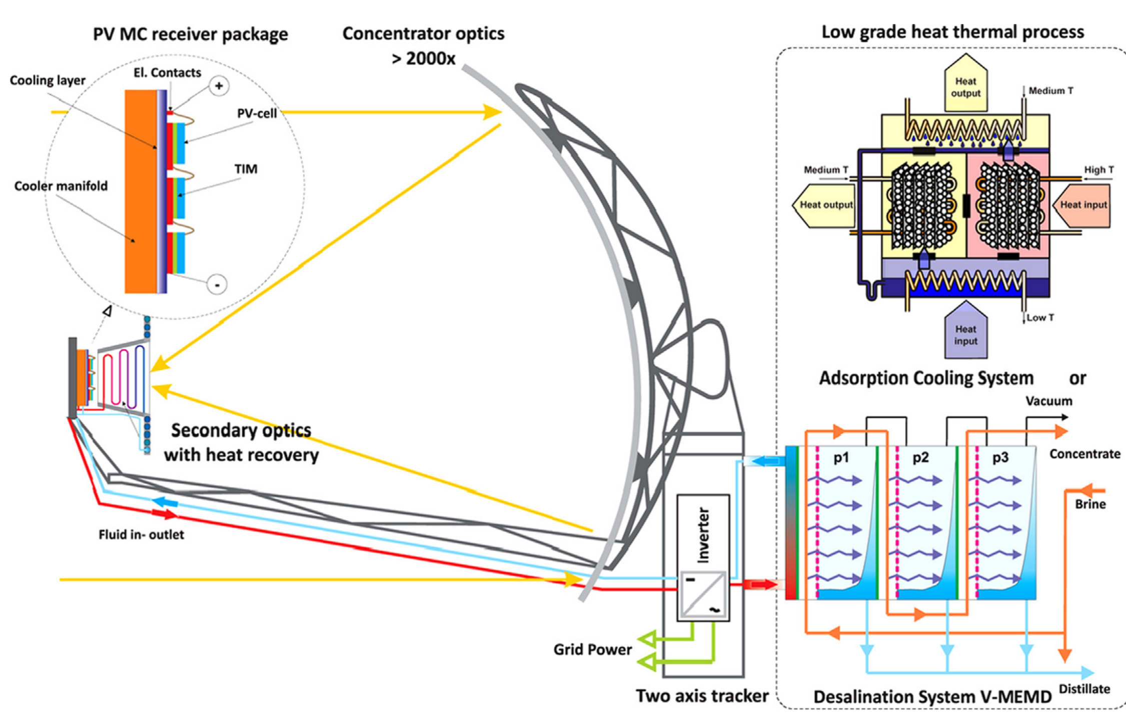


Fig. 1. Overview of HCPVT system with heat recovery for low grade thermal applications adsorption cooling (top right) and membrane distillation desalination (bottom right). Triple junction photovoltaic chips are mounted as an array on a multichip receiver (inset top left).

4. The model

4.1. Transmission system (HCPVT-adsorption cooling)

This section presents the modeling approach for the HCPVT system with adsorption cooling as the thermal end user. The system is expressed through a network composed of nodes and transmission lines. Each system component is referred to as a node (N1–N5) connected with different thermal loops (1–4). As illustrated in Fig. 2, the transmission system is comprised of four different thermal loops namely (1) interconnection of the collector area with the heat storage, (2) heat storage with the adsorption chiller, (3) adsorption chiller and cold storage, and (4) cold storage with end users (city). The hot storage is a layered tank which uses temperature gradients through the steady addition of water. Such condition is useful to prevent the exergetic destruction within the layered water tank. For this reason, hot water is fed into the top of the layered storage tank.

The characteristics of each transmission line are shown in Table 1.

The pipe diameters were dimensioned for a flow velocity in the range of 1.5 m/s, using commercially available casted iron pipes. Moreover, the pumping power was limited to less than 1% of the transported thermal energy, whereas, it can be seen that in the different piping sections the maximum is 0.1% for the long distance network. This simple approach enables the use of exergoeconomics [67] of the transmission system. The application of exergoeconomics is an elegant translation of the thermodynamic value of heat into a monetary unit. The relation between the rate of exergy derived from heat and its costs is reflected in the amount of exergy needed to produce the thermal output. This thermodynamic property (exergy) of heat is low and describes the maximum useful work gained through conversion. Therefore, the exergy content of low grade heat is more costly than the exergy content of electricity [68]. Transmission losses are included in the model to express the fact that the exergy contend is reduced.

The total designed input power is 35 MW; this figure exhibits the nameplate capacity and is linked to the maximum output from the power plant, as depicted in Table 2. In this case, the peak thermal output is 25 MW while the peak electrical production is 10 MW. However, the total incoming energy per year depends on *DNI* values. In this study, model *DNI* data from Meteonorm for Hammam Bou Hadjar was used to derive fluctuations the total system output. This data is also useful to calculate the capacity factor (refer to Eq. (1)) which is as assessment of the degree to which the power plant can be utilized.

$$CF = \frac{t_{peak} \times DNI_{nom} \times A_l}{t_{max} \times DNI_{max} \times A_l} \times \eta_{th+el} = 36.75\% \tag{1}$$

According to Metenorm 7 database, the maximum number of sun hours (t_{max}) in Hammam Bou Hadjar is 14 h (June). The capacity factor (*CF*) computed for a HCPVT generating station (assuming constant collector area A_l) equals only to about 36.75% (refer to Eq. (1)). This value is useful to pin-down the capability of generation at full capacity depending on maximum number of sun hours (t_{max}), the direct maximal irradiance (DNI_{max}) and total solar collector area (A_l), compared to its actual energy production. The latter is the product of peak sun hours (t_{peak}), the direct nominal irradiance (DNI_{nom}) and the total solar collector area (A_l). In addition, the overall efficiency of the system 87.5% (η_{th+el}) provides a polished description

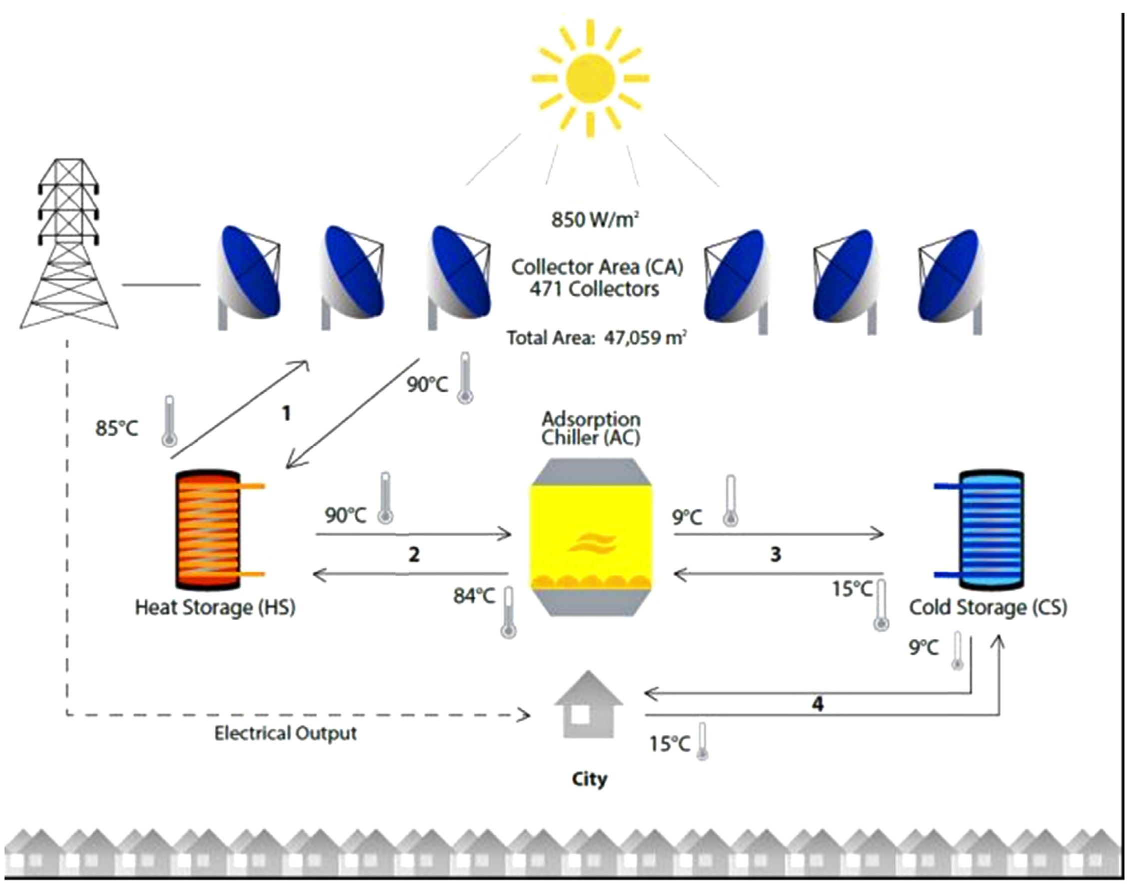


Fig. 2. Transmission system of a 10 MW HCPVT power plant with space cooling as thermal user. HCPVT with 10 MW electrical, 25 MW thermal output and a 24 h hot water storage (volume 6854 m^3). Space cooling is provided by an adsorption chiller and transport capacity is optimized by having a cold water storage with a 24 h capacity at the point of use (volume 1170 m^3).

Table 1
Thermal energy transmission network characteristics.

Loops	Length (m)	Transport diameter (m)	Mass flow rate (kg/s)	Pressure drop (bar)	Pumping power (kW)	Flow velocity (m/s)
1. CA to HS	11×1000	0.323	110	0.27	$11 \times 3.08 \geq 33.9$	1.38
2. HS to AC	2×500	0.813	996	0.08	$2 \times 8.2 \geq 16.4$	1.9
3. AC to CS	2×500	0.610	496	0.12	$2 \times 6.1 = 12.2$	1.7
4. CS to city	$2 \times 10{,}000$	1.0	496	0.24	$2 \times 11.7 \geq 23.4$	0.63

Table 2
Irradiance values, capacities and output for a simulated 10 MW HCPVT power plant in Hammam Bou Hadjar.

Population in Hammam Bou Hadjar	46,000
Averaged yearly *DNI*	2106 (kWh/m²yr)
Nominal peak irradiance (DNI_{nom})	850 W/m²
Maximum peak irradiance (DNI_{max})	984 W/m²
Peak sun hours (t_{peak})	6.8 h
Maximum sun hours (t_{max})	14 h
Nameplate capacity	40 MW
Designed capacity	25 MW_{th} and 10 MW_{el}
Electrical energy/yr	24,820 MWh
Thermal energy/yr	62,050 MWh
Pumping power	94.1 kW
Net el. generation	24,819 MWh_{el}

of the total revenues in the final valuation, since not all *DNI* can be converted to useful output. Even though this manuscript focuses mainly on the thermal system, the net present value was computed by taking into account the total electrical output of the HCPVT system.

The HCPVT electrical efficiency defined in Eq. (2) depends on the efficiencies of key components which were assumed to be 92% for the concentrator (tracking accuracy, primary optics), 93% for the secondary optics, 30% for the receiver module, and 98% for the inverter.

$$\eta_{el} = \eta_{concentrator} \times \eta_{s\ \ optics} \times \eta_{receiver} \times \eta_{inverter} \tag{2}$$

Consequently, thermal efficiency can be derived from Eq. (2) including the thermal collection efficiency of 94%.

$$\eta_{th,1} = \eta_{th,coll} \times \eta_{concentrator} \times (1 - \eta_{s\ \ optics} \times \eta_{receiver}) \tag{3}$$

Table 3 shows the assumed thermal efficiencies used in a nodal network for the most important components used in a 10 MW HCPVT power plant with heat reuse for space cooling.

Adsorption cooling features the lowest operating cost of all thermal cooling technologies due to its high electrical coefficient of performance (COP_{el}) and low maintenance [69,70]. A 50% average thermal efficiency ($COP_{th} = 0.5$) of the adsorption chiller in converting driving heat to useful cooling [71] was assumed and multiplied by the generated thermal power ($\dot{Q}gen$) which is 25 MW_{th}. The usable flow of thermal power ($\dot{Q}th$) for cooling is expressed by the following equation:

$$\dot{Q}_{th} = \dot{Q}_{gen} \times COP_{th} \tag{4}$$

While the internal electrical consumption of the adsorption chiller is negligible, the power requirement of the recooler for heat rejection must be taken into account. The electrical power required for the heat transfer fluid pump and fan motors was estimated at $\eta_{pump} = 0.6\%$ and $\eta_{fan} = 3.0\%$ of the rated recooler capacity, respectively [72]. This auxiliary power requirement for the adsorption chiller is represented by a single COP_{el}:

$$\dot{Q}_{el} = \frac{\dot{Q}_{gen}(1 + COP_{th})}{COP_{el}} \tag{5}$$

Table 3
Thermal efficiency table.

Name	Node	Assumed thermal efficiency (%)
Collectors	N1	62
Heat storage	N2	95
Adsorption chiller	N3	50
Cold storage	N4	95
Heat exchanger	N5	90

Table 4
Temperature gradients of the thermal network.

Loops	$(T_{in} - T_{out})$
1. CF to HS	90–85
2. HS to AC	90–84
3. AC to CS	15–9
4. CS to city	15–9

where $COP_{el} = (\eta_{pump} + \eta_{fan})^{-1}$ and $\dot{Q}_{el}$ is the estimated electrical power consumption of the recooler unit of the adsorption chiller.

Different methodologies had been used in the calculation of the overall system efficiency. Moran and Shapiro [73] illustrate it as the relation among the multi-carrier efficiencies:

$$\psi = \eta_{th,1} \times \eta_{th,ex} + \eta_{el} \tag{6}$$

The overall thermal efficiency of the HCPVT system 62.5% ($\eta_{th,1}$) and the electrical efficiency is 25% (η_{el}). The second-law efficiency $\eta_{th,ex}$ is computed by the Carnot efficiency ($1 - T_{ref}/T_{high}$), which for 90 °C hot water outflow and 30 °C ambient temperature is 16.5%. Hence, the overall system's exergetic efficiency is 35.3%. Through the combination with an adsorption chiller the heat output can be converted to a cold stream of economic value which is analyzed in four scenarios further below.

This model takes into account the net rate of enthalpy outflow (thermal energy plus flow work) [74] for the fluid flowing through each thermal loop. Eq. (7) expresses the difference in enthalpy for a constant mass flow rate, illustrated in $c_p(T_{in} - T_{out})$. The heat flow through the tubes is:

$$\dot{Q} = \dot{m} \times c_p \times \Delta T \tag{7}$$

The heat flow is dependent on the rate of mass transported through the pipe $\dot{m}$, the specific heat capacity c_p and the temperature gradient ΔT. The temperature gradients in the different network sections are depicted in Table 4.

5. Exergoeconomic analysis

The use of the second law of thermodynamics has been widely used in economics [75], especially after the 1990s. Major contributions

were written by Tsatsaronis [76] and Erlach et al. [77]. Tsatsaronis introduced the term “exergoeconomics” and developed its application in the field of industrial processes. The exergoeconomic analysis anchors its assessment in the cost analysis of processes. This blends with the evaluation of fixed, variable and capital costs within the system. To understand the fundamental mechanisms of exergy in the transmission system we look at following physical properties of the water: the density (ρ), specific heat capacity (c_p) and dynamic viscosity (μ) respectively.

All three contributions are temperature dependent (see Fig. 2 for the water's reference temperatures along the pipes). These parameters are necessary to calculate the mass flow rate, the mean velocity, friction factor for turbulent flow, pressure drop and pumping power within each section of the fluid network. For $Re > 2300$, the Fanning's friction factor [74] depends on Reynold's number and may be approximated by:

$$f_{fanning} = 0.079\mathrm{Re}^{-0.25} \tag{8}$$

The interaction between the fluid and wall of the pipe are useful to outline the geometry and design of each transmission line. The thermal loop goes through a hot and cold storage and through the adsorption chiller. All of these components need a pump to transfer the fluid along the pipes. To find the net generation, the energy consumption of each pump needs to be discounted from the final electricity output. We sequentially define the equations to derive the rate of electrical power consumed by each pump along the system.

The volumetric flow rate ($\dot{V}$) depends on a cross-sectional area (A_{pipe}) of the pipe and the fluid's mean velocity (v):

$$\dot{V} = A_{pipe} \times v \tag{9}$$

Subsequently, the mass flow rate ($\dot{m}$) is introduced to describe the amount of water that will be discharged from the hot and cold water storage tank (refer to Eq. (7)). As the fluid density varies with temperature, the velocity of the fluid varies over the cross-sectional area of the pipe. Under steady state conditions, the mean velocity flow velocity in the pipe can be evaluated according to the following equation:

$$v = \frac{\dot{m}}{\rho \times A_{pipe}} \tag{10}$$

Finally, it should be outlined that the pressure drop and pumping power depend on the geometry of the tubes. In our formulation, the pressure drop does account for temperature dependent variable thermo-physical properties of the fluid but for contraction and expansion of the pipes. The pressure drop is summarized as

$$\Delta p = \frac{2 \times f_{fanning} \times \rho \times v^2 \times L}{D_{pipe}} \tag{11}$$

where L refers for the length of the pipe, $f_{fanning}$ is Fanning's friction factor, v^2 is the squared velocity, D_{pipe} is the pipe's diameter and ρ is the density of the fluid.

Doubling the flow velocity will increase the pressure drop by a factor of 4. This will increase the electricity consumed by the pump:

$$\dot{Q}_{pump} = (\Delta p \times \dot{V}) \tag{12}$$

Since the volumetric flow rate ($\dot{V}$) also depends on the velocity, doubling the volumetric flow rate will increase pumping power by 8 fold. The results are illustrated in Table 1. Adding up the pumping power from the different thermal loops we get 2.37 MWh pumping energy needed to transport the produced thermal energy per year. Hence, the net generation is found by subtracting pumping losses to the electrical generation.

6. Storage

The model considers different loops within the HCPVT power plant. The first loop reflects the link among 471 ground mounted collectors, needed to produce 25 MW_{th} and 10 MW_{el}. The tubes have a predefined diameter and length depending on the pressure drop and resistances. The purpose of this loop is to transfer the fluid at 85 °C to the cooling loop of each single HCPVT collector and gather the generated thermal energy at the receiver module and secondary optics. Subsequently, the water will be delivered back to the heat storage tank at a temperature of 90 °C. This thermal yield allows heat utilization for space cooling activities. In addition the lifetime of the receiver is also improved if it can be operated with low thermal gradients. In contrast to air cooled CPV systems which operate with a higher thermal gradient.

Heat demand for space cooling activities increase when ambient temperature differs from the reference temperature. Therefore, the amount of heat to be stored entangles two different dimensions, a technical and an economic one. The technical dimension of the 24 h heat storage volume (VHS) is illustrated below:

$$VHS = \frac{[((Q_{gen} \times 10^6) \times t_{peak}) \times 3600]}{(c_p \times \Delta T)} \times \frac{24}{t_{peak}} \tag{13}$$

Both heat and cold storage represent one of the biggest advantages of the HCPVT station. The heat storage allows a 24 h operation of the adsorption chiller thereby compensating the intermittent nature of solar radiation. The cold storage ensures quality of supply encompassing the flexibility of a spinning reserve. This is a competitive advantage when compared with other PV systems. In the near future, renewable technologies will exert an increasing influence in space cooling and heating activities [78]. However, for an efficient development of the HCPVT system, trends in thermal demand for space cooling activities need be considered.

As already mentioned, 25 MW represents the thermal capacity of the first and second loop. However, the adsorption chiller is characterized by an average thermal COP of 0.5. Thus, after passing through the adsorption chiller, the cooling power of the third and fourth loop is equivalent to 12.5 MW. Therefore, the capacity of the cold storage has to be set according to the system efficiencies and the cooling energy consumption delivered in the simulation.

Each loop operates with a ΔT of 6 K. However, the first loop operates with a ΔT of 5 K to allow a more efficient reuse of the heat extracted from the active cooling. The hot storage needs an approximate volume of 6854 m^3 to secure a 24 h operation. Storage capacity can help to reduce the size of the system while still being able to cover peak cooling demand. Storage to cover extended periods of cloudy weather is not needed because cooling demand during these periods is also smaller.

To enhance flexibility and to reduce the transport cost, the storage tank should be large enough to guarantee at least 24 h storage. The peak sun hours in Hammam Bou Hadjar are 6.8 h (t_{peak}) calculated with a nominal irradiance of 850 W/m^2 (DNI_{nom}) which provides a total daily average thermal energy (E_{th}) of 170 MWh for the 25 MW thermal power of the HCPVT system. The thermal efficiency ($\eta_{th,1}$) is defined as 62.5% for node N1. With a total collector area of 47,059 m^2 (A_l), the annual gross thermal output is 62,050 MWh.

$$E_{th} = (t_{peak} \times DNI_{nom} \times A_l) \times \eta_{th,1} = 170\ \mathrm{MWh/day} \tag{14}$$

The economic dimension concerning the volume of the heat storage represents the energy consumption used for activities such as space cooling. The reference temperature maps the preferred range in temperature which determines the underlying heat consumption for space cooling. This is both, a useful concept

in normative economics to follow the "doctrine of consumer sovereignty" (meaning consumers command the economy), and to simulate heat consumption in a certain region to tune production efficiently.

The thermal activity should be viewed as a durable good which yields a certain utility over time. Thus, the reference temperature represents a utility enhancing condition. In welfare economics, the so called "social welfare" refers to the aggregation of "cardinal" individual utility curves. This paper focuses on individual utility in Hammam Bou Hadjar, and neglects the evaluation of interpersonal utility.

According to Alberini and Filippini, "household appliances and lighting consumes approximately 45% of the energy in a typical household, whereas space heating, water heating and air conditioning account for 30%" [79]. To construct the benchmark thermal demand function, Cooling Degree Days (CDD), average living surface, insulation and the average price of electricity are adopted. To avoid correlation among explanatory variables income per capita is not considered, i.e. between size of the apartment and income. Polysun's benchmark thermal demand is depicted in Eq. (16).

$$D_{th} = \left[\varphi \sum_{i=1}^{24} CDD\right]\left[1+\varepsilon\left(\frac{P_{th}}{P_{el}}-1\right)\right] \tag{15}$$

Eq. (15) highlights the inverse relation between prices (P_{el} 0.06 USD/kWh [80] and P_{th} 0.018 USD/kWh) and demand. Technologically a similar price can be derived since a COP of a compression cooler is about 3.3.

Elasticity (ε) of demand depicts the relation between price and demand patterns in a specific region. Note that ε is exogenous and represents the average elasticity of demand taken as a constant ($\varepsilon = 0.8$) for cogenerating station. This means if price increases by 1% demand for energy decrease by 0.8%. Cooling is considered a "high end" product in Algeria while electricity is not. In fact, high end products are linked to income. Countries with high GDP per capita will consume more "high end" products than low income countries. A vast number of publications had reported that energy demand is inelastic in the short run but more elastic in the long run.

Table 5
Building specific features.

Bulding features	Value	Unit
U-value of building (k)	0.8	W/(K m²)
Length of building	15	m
Width of building	10	m
Average living surface (A)	150	m²
Specific cooling energy demand per year	65.9	kWh/m²
Number of people per dwelling (N)	4	–

The equation projects the simulation run in Polysun where φ is a function of insulation (k), average living surface (A) and average number of people (N) in the dwelling, expressed as

$$\varphi = f(A, k, N) \tag{16}$$

The assumed values are shown in Table 5. The heat loss coefficient or U-value of the building was set to 0.8 W/(m^2 K). The latter determines energy conservation and defines how ambient temperature filters through the living surface, affecting its temperature Table 6.

7. The cost function

The total cost function is a function of output quantities, that illustrates both fixed and variable costs. To estimate total costs and assess the profitability of the HCPVT plant, fixed costs are taken as time dependent. Fixed costs are represented by overhead costs and insurance. Variable costs are those expenses changing as function of production and are also referred as operating expenditure (OPEX). Operation and maintenance was assumed to represent 75% of the variable costs. In our model however, capital is considered fixed.

The cost associated with the collector reflects a bulk acquisition from its different components. The breakeven point is reached if total revenues are equal or greater than the total cost of thermal generation.

The integration of the net present value (NPV, refer to Eq. (17)) adds transparency in the investment decision. The NPV is a function of future cash flows and the cost of capital (i). The discount is valid for every receipt (R) and expenditure (E) over the plant's lifetime (25 years). Furthermore, the expenditures are discounted over a 6% rate which is in accord with IMF lending rates for development projects which range from 5.75% to 6% per year [81]. Expenditures include fixed and variable costs. Nonetheless, just variable costs are discounted per annum. The benchmark demand of electricity for Hammam Bou Hadjar is part of the receipts and so is the price. However, the 10 MW power station can only cover 52% of the electrical demand of the region. In addition, the total thermal output is also part of the incoming revenues, assuming supply equals demand. The amount of receipts yielded by the deployment of the generating station is multiplied by the growth rate (g). The latter illustrates exogenous variables such as population growth and the increase in electricity consumption per capita over one year. According to the IMF, annual population growth in Algeria is about 1.5% and electricity consumption per capita increases at 1% per year. However, a general approximation can also be made by using real GDP growth across the Algerian economy.

Table 6
Summary of results for different scenarios.

Scenario 1	49,728 MWh	This amount shows the minimum output quantity that needs to be sold per year at a thermal price of 18 USD/MWh. This scenario also considers electricity prices in Algeria to be 60 USD/MWh as the costs involve electricity and thermal generation. The figure expresses the relation between fixed costs and the marginal profit.
Scenario 2	10.92%	Economic growth rate of a country necessary to breakeven over a 25 year period. The thermal COP for adsorption cooling is taken into account taking the overall thermal output level from 62,050 MWh/yr (heating) to 31,025 MWh/yr (cooling).
Scenario 3	14 USD/MWh	Assuming a jump in the COP from 0.5 to 0.7 the final thermal output increases from 12.5 MW to 17.5 MW (cooling). The equilibrium price is 14 USD/MWh assuming a zero profit condition in year 11.
Scenario 4	0%	Assuming the ideal cooling consumption per year, 0% represents the economic growth rate needed to have a $NPV = 0$ over a 25 year period. This simply illustrates the fact that receipts are greater than expenditures.

The *NPV* is of the form

$$NPV = \frac{\sum_0^T R_t (1+g)^t}{(1+i)^t} - \frac{\sum_0^T E_t}{(1+i)^t} \tag{17}$$

Economic growth has been explained by many research groups. They proclaim its foundation is fueled by different factors, such as population density, technological progress, human capital, total factor productivity [83] and trade. In this model, the rate of technological progress is embedded in the increasing efficiency of replacing components in a HCPVT station. The adsorption chiller is expected to have a life expectancy of 10 years. Therefore, the model assumes the replacement of the adsorption chiller in 10 years.

8. Scenario analysis

This takes us to the analysis and development of four different scenarios to answer following questions:

1. When is the profit equal to 0 and how does it evolve?
2. At which growth rate is the *NPV* going to be equal to 0?
3. In case there is a replacement of different components how are output and costs evolving over time?
4. A simulation reports the total yearly potential thermal consumption. At which growth rate the *NPV* is equal to 0?

The model aims to describe under which scenarios the *NPV* is turning positive and how demand evolves over the plant's lifetime. The first scenario captures the minimum output quantities that need to be sold per year. As a first step, a zero profit condition is set depicting the break-even set of observations under the total cost curve. For simplicity, the production side is characterized by a zero profit (π) environment, i.e. total revenues equal total costs:

$$\pi = P \times D - C = 0, \quad \text{with } C = \beta + \gamma \times D \tag{18}$$

After some rearranging we find the demand function:

$$D = \frac{\beta}{P-\gamma} \tag{19}$$

where P is the price and β are fixed costs. The marginal profit is illustrated as $(P-\gamma)$, and indicates the profit per extra unit of output. This implies an overall loss can also be experienced in case variable costs (γ) are too large. Since this paper focuses on a co-generating station, total costs reflect the production of both, electricity and thermal power. For this reason we use electricity prices to be 60 USD/MWh [79] and thermal prices to be 18 USD/MWh. This zero profit condition shows that the yearly quantity which needs to be sold to break-even is 49,728 MWh. Therefore, break-even can be seen as a possible option since this quantity is lower than the total amount of energy that the HCPVT power station can produce per year.

The supply perspective bundles the net present value of the proposed power plant fixed (β) and variable costs. Fixed costs are the sum of overhead costs and insurance. These are considered independent of output. On the contrary, variable costs, such as O&M, are subject to fluctuations and depend directly on the final output. An increase in output can be related to different variables. As expressed in Solow's Growth Model, the amount of output rises each period if technological efficiency increases. Technological progress can also be viewed from a multidimensional array, where the cost perspective is also included. However, the increasing efficiency of solar cells, optics and the adsorption chiller in each period have a direct effect on the final output and on the average total costs of production. In contrast, economies of scale are achieved given an inverse relation between output quantities and production costs. This is reflected at the minimum point of average costs.

The second scenario reports the growth rate needed for the *NPV* to breakeven assuming that the overall electrical and thermal demand of Algeria according to the World Bank are satisfied [84]. The calculation is performed by varying the growth rate while keeping all other variables fixed. Therefore, demand equals supply taking the thermal and electricity price at 18 USD/MWh and 60 USD/MWh. The thermal output is reduced by the thermal *COP* (0.5) of the adsorption chiller. The scenario suggests that this type of power plants should be placed in countries with high growth rates and high initial levels of income.

The third scenario is computed to evaluate the economic relation between the COP_{th}, the costs and the final thermal output (E_{th}). We assume an increase in the adsorption chiller efficiency which strongly affects the rate of generation per unit of peak sun hours (6.8 h) and nominal irradiance.

$$E_{th} = (t_{peak} \times DNI_{nom} \times A_l) \times (\eta_{th,1} \times COP_{th}) \tag{20}$$

Appearance of a COP_{th} equal to 0.7 is attributed to a sharp technology improvement which accompanies a considerable cost reduction over the years. The equation equals to a daily net cooling output of 119 MWh.

The function P accounts for the breakeven price at which thermal output should be sold given a zero profit condition. It assumes an equilibrium condition in which demand equals supply in a specific period of time. Variable costs (γ) are discounted at an inflation rate of 7% to highlight the inter-temporal state of the model.

$$P = \frac{\pi - (\beta + (\gamma \times D))}{D_{t+1}} \tag{21}$$

The quantity demanded in $t+1$ is

$$D_{t+1} = [E_{th} \times 365] \times (1+g)^{11} \tag{22}$$

The growth rate (g) is 2.5% per year. It illustrates the increasing rate of thermal energy demanded per year and is multiplied with the thermal generation. Hence, the quantity demanded should be in the range of 56,990 MWh/yr. However, fixed and variable costs represent a bulk amount accounting for 10 years. Therefore, the quantity demanded in $t+1$ should be multiplied by the amount of years. Afterwards, the price can be calculated per year. Under this economic configuration the equilibrium price is 14 USD/MWh in the 11th year. Unlike the electricity market, the heat market is not established yet in Algeria. However, even if there is no market for heat we can estimate the minimum price based on the evolvement of costs over time.

The fourth scenario reports the potential demand given Hammam Bou Hadjar's weather conditions. It adopts utility on an aggregate basis assuming full adoption of cooling at a 22 °C reference temperature. The simulation of heat consumption rates (for space cooling activities) is subject to Cooling Degree Days (*CDD*) in Hammam Bou Hadjar, the average area and specific building features as shown in Table 5.

The yearly cooling demand for a model household was 65.9 kWh/m² in Hammam Bou Hadjar. The monthly cooling demand variability is illustrated in Fig. 3.

Fig. 3 summarizes the simulated cooling demand results. It is stated that the yearly effective cooling delivered to a model household is 19,490 kWh. Monthly results spur clarity on the cooling demand variation depending on seasonal temperature differences, i.e. actual minus reference temperature. Therefore, 19,490 kWh represents 3 times more the overall (gross) cooling output (62,050 MWh) of the HCPVT multi-carrier generating power plant. Therefore this plant

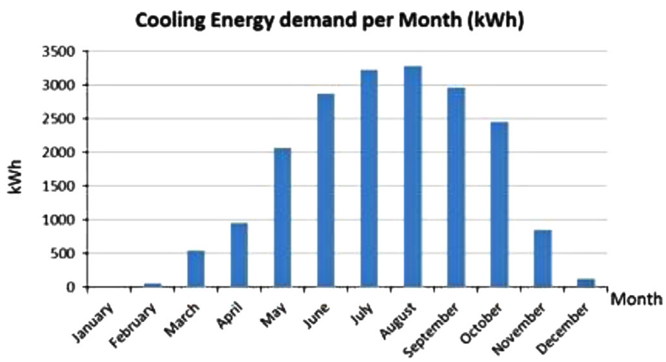


Fig. 3. Monthly cooling energy demand in Hammam Bou Hadjar.

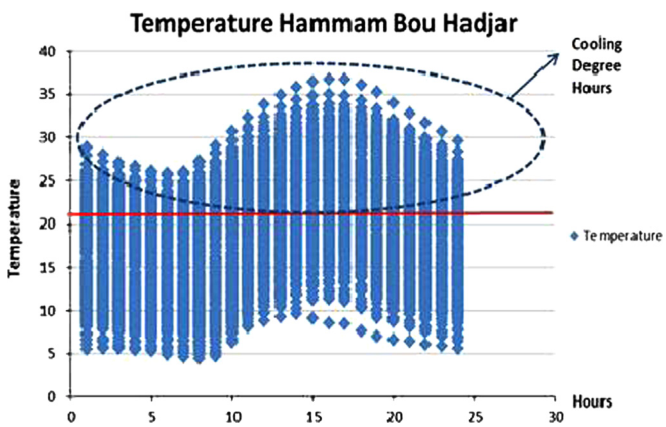


Fig. 4. Annual temperature data in Hammam Bou Hadjar for the Cooling Degree Day calculation.

could cover the cooling demand for about 3200 households or 12,500 out of the 46,000 inhabitants.

For simplicity reasons we assume a specific cooling energy demand per average household (4 people) of 19,490 kWh as the yearly aggregate level of thermal consumption.

To grasp the difference between electricity prices and heat prices a proper disaggregation of electricity consumption is needed. However, it is difficult to make a distinction between a change in relative prices due to inflation and other economic parameters. As already mentioned, both thermal and electricity demand have to be decomposed to find the weight a consumer assigns to the thermal and electrical output. Therefore, the quantity demanded depends on electricity prices, income and preferences. Preferences are linked to the reference temperature which determines the comfort in the ambient temperature level of the household. A widespread number of papers [79,85], made reference to the response on electricity demand to prices. To capture seasonal demand variations weather data is extracted from Meteonorm to calculate *CDD*.

The computation of *CDD* [82] is based on the hourly temperature in Hammam Bou Hadjar (T_i) and a reference temperature (T_{ref}) of 22 °C. *CDD* are represented as

$$CDD = \frac{\sum_{i=1}^{24} (T_i - T_{ref})_{T_i > T_{ref}}}{24} \qquad (23)$$

Fig. 4 shows the daily maximal and minimal temperatures in Hammam Bou Hadjar. The area above 22 °C represents the *CDD* which affect the thermal cycle in an average household.

Even if these figures could give a good approximation of thermal cycles in Hammam Bou Hadjar, it neglects “day-type” [60] assumptions necessary for short-term load forecasting.

Finally, the fourth scenario aims to determine the difference between electrical and cooling consumption. We follow a simple approach where thermal power accounts for 30% in a household whereas electrical appliances account for 45% [79]. Therefore, the price for the thermal output is 18 USD/MWh. Using the *NPV*, the growth rate needed to breakeven is 0%. This is because the sum of electrical output sold at 60 USD/MWh and the potential thermal output sold at 18 USD/MWh is higher than the overall expenditures of an HCPVT power station (10 MW_{el} and 25 MW_{th}). Obviously, this is the ideal scenario; in reality countries with high GDP growth are more suitable for this kind of power stations. Countries with high per capita income should be considered as space cooling is often seen as a luxurious service. In fact, cooling requires a higher amount of energy. One indicator to be considered is GDP's growth rate in the country where the thermal user is going to be placed. In fact, the Algerian GDP growth rate ranges from 2.5–3% p.a., whereas Morocco's GDP fluctuated from 3.7 to 4.5% in the last 3 years; echoing the possibility of higher living standards. In addition, economic development spurs knowledge on energy use per country. In fact, the proper GDP breakdown of the energy sector leads to a better understanding of seasonality variations in energy consumption per country.

The GDP per capita in Algeria for 2012 was USD 7500 [86]. Therefore, average electricity consumption in Algeria accounts for 0.82% of total income, reflecting low electricity prices. According to the World Bank, Algeria's electricity consumption per capita is higher than that of Morocco (0.781 MWh) but lower than that of Tunisia (1.350 MWh). Hence, using the potential average cooling demand data from the simulation, cooling expenditures can be inferred being ~1% of total income. However, this represents the ideal cooling point or maximum comfort an individual can get. According to this scenario, individuals will cool down their apartment whenever 22 °C are exceeded.

The results for the different scenarios are given in Table 6.

Future work could be based on a different price assumption. It can take the price of solar power as the ratio expressed by the cost and the total thermal output per area. The cost per area includes those expenses incurred from collector, balance of system (BOS, that includes wiring, building the cement frame and ground-mounting the collector), transmission system and the final installation. Price components can be reduced either by increasing the efficiency of some of the system's components (driven by technological progress) or because of the exploitation of economies of scale. However, installation and balance of systems costs are difficult to reduce. Therefore, it can explain where system costs can be driven down if a price reduction takes place for individual collector components or the adsorption chiller.

9. Conclusions

The project appraisal illustrates a dissection of the system to value the investment under a discounted basis. The results of the technical and economic analysis show how to optimize the HCPVT power plant for a specific location, in this case for Hammam Bou Hadjar, Algeria, and to determine the value of heat. The thermodynamic property (exergy) of heat is low and describes the maximum useful work gained through the conversion of heat to cooling. Therefore, production costs per unit of thermal output are higher compared to other energy carriers. For space cooling activities the costs strongly depend on the costs of solar collectors and the adsorption chiller *COP*. If the costs for space cooling were to come down given higher *COP* and specific cooling power (*SCP*) values, a more competitive cost structure could be expected. An increasing amount of renewable and cogenerating stations may emerge in the future.

For many other reasons space cooling demand is bound to increase. However, space cooling is a luxurious product, especially in low and middle income countries. Increasing technological improvements such as HCPVT stations would allow heat reuse on a widespread basis. A higher level of granularity reveals the real plant's generation through the involvement of exergy. Production costs reflect temporal and spatial evolvement of thermal distribution, showing the relationship among, efficiencies, the capacity factor, and the exergy. Transporting the energy through a water piping system could reduce electric grid congestion in regions with high space cooling demand or other thermal activities. Therefore, it can add diversification through a new transmission and distribution system, deferring the need for additional transmission lines. Small-scale distributed power generation can be placed close to inflexible loads or in the immediate vicinity around congested zones. The HCPVT generating station enables flexibility through a 24 h thermal storage; so that when the sun is not shining the demand can be satisfied through the depletion of the cold and hot storage. This allows an enhanced competitiveness over the years, particularly when economies of scale and the efficiencies of different system components increase. The results show the equilibrium price of 14 USD/MWh when the first law thermal efficiency increases (scenario 3).

Four different scenarios were analyzed reporting the effects on *NPV*, efficiencies, growth rates and prices. For scenario 1 a break-even can be reached as the produced quantity (62,050 MWh for thermal power and 24,817 MWh for electrical power) is higher than the break-even quantity of 49,728 MWh. In equilibrium, scenario 2 evaluates the demand using the thermal and electrical output, respectively. It also compares it with the benchmark demand taken from the World Bank to figure out how much of the electrical and thermal demand can be covered by net generation. Break even can be achieved at a 10.92% growth rate. While scenario 2 uses a demand derived from the generating output, scenario 4 measures potential thermal demand based on a simulation ran in Polysun. This unfolds the differences between electricity and thermal demand in Hammam Bou Hadjar. Both scenarios report the required growth rate per year to reach breakeven. For scenario 4 0% is needed as receipts are higher than the expenditures. This determines the curtailment of viewing countries with high economic growth rates. Algeria is classified as a middle income country with high *DNI*, and a great potential for cooling demand growth. However, space cooling can be seen as a “high end” product, meaning its consumption depends on income. This was the main motivation to use the elasticity of demand based on a benchmark price of electricity in Algeria and compared it with a potential thermal price. However, we expect a decrease in the elasticity of demand since cooling demand and technological improvement in PV technologies are expected to take place. In the long run increasingly efficient renewable technologies are going to play a key role in the energy market. These developments will change the dynamics of the energy market expanding the horizons of the thermal market. The HCPVT station shows the potential to deploy solar energy and heat at reduced costs.

The fast technological innovation in the field of renewables creates a demand for economical analyses, in particular when co-generation is involved and when new technologies have to be compared to existing infrastructures. We demonstrated that an exergo-economic analysis is a useful tool in Algeria and we believe this analysis can be performed for any area for which *DNI*, Cooling Degree Days (*CDD*), average living surface, insulation, the average price of electricity and the power plant technical aspects are known. Using the analysis in countries that exhibit transparency in energy prices for a larger number of years would even allow obtaining more accurate predictions.

References

[1] Renewable Energy Policy Network for the 21st Century (REN21). Renewables. Global Status Report 2012. 〈http://www.map.ren21.net/GSR/GSR2012_low.pdf〉; 2012.

[2] Kurtz S. Opportunities and challenges for development of a mature concentrating photovoltaic power industry. National Renewable Energy Laboratory. Technical Report. 〈http://large.stanford.edu/courses/2010/ph240/kalantarian1/docs/43208.pdf〉; 2009.

[3] Hernandez- Moro J, Martínez-Duart JM. Analytical model for solar PV and CSP electricity costs: present LCOE values and their future evolution. Renew Sustain Energy Rev 2013;20:119–32.

[4] Branker K, Pathak MJM, Pearce JM. A review of solar photovoltaic levelized cost of electricity. Renew Sustain Energy Rev 2011;15:4470–82.

[5] Darling SB, You F, Veselka T, Velosa A. Assumptions and the levelized cost of energy for photovoltaics. Energy Environ Sci 2011;4:3133–9.

[6] Solanki CS, Sangani CS. Estimation of monthly averaged direct normal solar radiation using elevation angle for any location. Sol Energy Mater Sol Cells 2008;92:38–44.

[7] Hering G. Loosing steam? Photon Int, Sol Mag 2012:74–89.

[8] Wolf M. Performance analyses of combined heating and photovoltaic power systems for residences. Energy Convers 1976;16(1):79–90.

[9] Kern EC, Russell MC. Combined photovoltaic and thermal hybrid collector systems. In: Proceedings of the 13th IEEE photovoltaic specialists; 1978. p. 1153–7.

[10] Florschuetz LW. Extension of the Hottel–Whillier model to the analysis of combined photovoltaic/thermal flat plate collectors. Sol Energy 1979;22(4):361–6.

[11] Nakata Y, Kobe T, Shibuya N, Machida T, Takemoto T, Tsuji TA. 30 kWp concentrating photovoltaic/thermal hybrid system application. In: Proceedings of the sixteenth IEEE photovoltaic specialists conference; 1982. p. 993–8.

[12] Chow TT. A review on photovoltaic/thermal hybrid solar technology. Appl Energy 2010;87(2):365–79.

[13] Singh B, Othman MY. Review on photovoltaic thermal collectors. J Renew Sustain Energy 2009;1(6):062702.

[14] Joshi AS, Dincer I, Reddy BV. Performance analysis of photovoltaic systems: a review. Renew Sustain Energy Rev 2009;8(13):1884–97.

[15] Du D, Darkwa J, Kokogiannakis G. Thermal management systems for photovoltaics (PV) installations: a critical review. Sol Energy 2013;97:238–54.

[16] Akbarzadeh A, Wadowski T. Heat pipe-based cooling systems for photovoltaic cells under concentrated solar radiation. Appl Therm Eng 1996;16(1):81–7.

[17] Luque A, Sala G, Arboiro JC, Bruton T, Cunningham D, Mason N. Some results of the EUCLIDES photovoltaic concentrator prototype. Prog Photovolt: Res Appl 1997;5(3):195–212.

[18] Sala G, Anton I, Arboiro JK, Luque A, Camblor E, Mera E, et al. The 480 kW EUCLIDES-thermie power plant: installation, set-up and first results. In: Proceedings of the 16th European photovoltaic solar energy conference; 2000. p. 2072–7.

[19] Ito S, Miura N, Wang K. Performance of a heat pump using direct expansion solar collectors. Sol Energy 1999;65(3):189–96.

[20] Coventry JS. Performance of a concentrating photovoltaic/thermal solar collector. Sol Energy 2005;78(2):211–22.

[21] Kribus A, Kaftori D, Mittelman G, Hirshfeld A, Flitsanov Y, Dayan A. A miniature concentrating photovoltaic and thermal system. Energy Convers Manag 2006;47(20):3582–90.

[22] Mittelman G, Kribus A, Dayan A. Solar cooling with concentrating photovoltaic/thermal (CPVT) systems. Energy Convers Manag 2007;48(9):2481–90.

[23] Li M, Li GL, Ji X, Yin F, Xu L. The performance analysis of the trough concentrating solar photovoltaic/thermal system. Energy Convers Manag 2011;52(6):2378–83.

[24] Charalambous PG, Maidment GG, Kalogirou SA, Yiakoumetti K. Photovoltaic thermal (PV/T) collectors: A review. Appl Therm Eng 2007;27(3):257–86.

[25] Handy J, Peterson T. Concentrating PV survey: an unbiased overview. In: Proceedings conference on high and low concentrator systems for solar electric applications VI; 2011. p. 1–11.

[26] Chemisana D. Building integrated concentrating photovoltaics: a review. Renew Sustain Energy Rev 2011;15:603–11.

[27] Tiwari GN, Mishra RK, Solanki SC. Photovoltaic modules and their applications: a review on thermal modeling. Appl Energy 2011;88(7):2287–304.

[28] Calise F, Dentice d'Accadia M, Vanoli L. Design and dynamic simulation of a novel solar trigeneration system based on hybrid photovoltaic/thermal collectors. Energy Convers Manag 2012;60:214–25.

[29] Vivar M, Clarke M, Pye J, Everett VA. Review of standards for hybrid CPV-thermal systems. Renew Sustain Energy Rev 2012;16(1):443–8.

[30] Hinrichs D. Cogeneration. Reference module in earth systems and environmental sciences. Encycl Energy 2004;1:581–94.

[31] Hernandez-Santoyo J, Sanchez-Cifuentes A. Trigeneration: an alternative for energy savings. Appl Energy 2003;76(1–3):219–27.

[32] Tonui JK, Tripanagnostopoulos Y. Air-cooled PV/T solar collectors with low cost performance improvements. Sol Energy 2007;81(4):498–511.

[33] Coventry SJ, Lovegrove K. Development of an approach to compare the ‘value’ of electrical and thermal output from a domestic PV/thermal system. Sol Energy 2003;75(1):63–72.

[34] Yu Vorobiev, Gonzalez-hernandez J, Vorobiev P, Bulat L. Thermal–photovoltaic solar hybrid system for efficient solar energy conversion. Sol Energy 2006;80(2):170–6.

[35] Tiwari A, Sodha MS, Chandra A, Joshi JC. Performance evaluation of photovoltaic thermal solar air collector for composite climate of India. Sol Energy Mater Sol Cell 2006;90(2):175–89.
[36] Bosonac M, Sorensen B, Katic I, Sorensen H, Nielsen B, Badran J. Photovoltaic/thermal solar collector and their potential in Denmark. Final report EEP project 1713/00-0014; 2003. p. 28.
[37] Joshi AS, Dincer I, Reddy BV. Thermodynamic assessment of photovoltaic systems. Sol Energy 2009;83(8):1139–49.
[38] Agrawal Sanjay, Tiwari GN. Energy and exergy analysis of hybrid microchannel photovoltaic thermal module. Sol Energy 2011;85(2):356–70.
[39] Mishra RK, Tiwari GN. Energy matrices analyses of hybrid photovoltaic thermal (HPVT) water collector with different PV technology. Sol Energy 2013;91:161–73.
[40] Raman V, Tiwari GN. Life cycle cost analysis of HPVT air collector under different Indian climatic conditions. Energy Policy 2008;36:603–11.
[41] Saidur R, BoroumandJazi G, Mekhlif S, Jameel M. Exergy analysis of solar energy applications. Renew Sustain Energy Rev 2012;16(1):350–6.
[42] Agrawal Sanjay, Tiwari GN. Exergoeconomic analysis of glazed hybrid photovoltaic thermal module air collector. Sol Energy 2012;86(9):2826–38.
[43] Deshmukh MK, Deshmukh SS. Modeling of hybrid renewable energy systems. Renew Sustain Energy Rev 2008;12(1):235–49.
[44] Ahmada S, Abidin MZ, Ab Kadirb, Shafiea S. Current perspective of the renewable energy development in Malaysia. Renew Sustain Energy Rev 2011;15:897–904.
[45] Mtshali TR, Coppez G, Chowdhury S, Chowdhury SP. Simulation and modeling of PV–wind–battery hybrid power system. In: Proceedings of the IEEE power and energy society general meeting, Detroit; 2011. p. 1–7.
[46] Dursun E, Kilic O. Comparative evaluation of different power management strategies of a stand-alone PV/wind/PEMFC hybrid power system. Electr Power Energy Syst 2012;34:81–9.
[47] Technology Roadmap Solar Heating and Cooling, International Energy Agency. 〈http://www.iea.org/publications/freepublications/publication/name,28277,en.html〉; 2012.
[48] Balaras CA, Grossman G, Henning HM, Infante Ferreira CA, Podesser E, Wang L, et al. Solar air conditioning in Europe—an overview. Renew Sustain Energy Rev 2007;11(2):299–314.
[49] Ong CL, Escher W, Paredes S, Khalil A, Michel B. A novel concept of energy reuse from high concentration photovoltaic thermal (HCPVT) system for desalination. Desalination 2012;295(1):70–81.
[50] Isaac M, van Vuuren DP. Modeling global residential sector energy demand for heating and air conditioning in the context of climate change. Energy Policy J 2009;37:507–21.
[51] Polysun Software Version 7 Package Vela Solaris, Switzerland.
[52] Rezaei SH, Witzig A, Pfeiffer M, Lacoste B, Wolf A. Modeling and analyzing solar cooling systems in Polysun. In: Proceedings of the 3rd international conference on solar air-conditioning. 〈http://www.polysun.ch/files/2009-10-otti-solarcooling-palermo.pdf〉; 2009.
[53] Meteonorm 7 from Meteotest, Switzerland.
[54] Görig M, Breyer C. Energy learning curves of PV systems. In: Proceedings of the 27th European photovoltaic solar energy conference; 2012. p. 4682–92.
[55] Kienzle F, Ahcin P, Andersson G. Valuing investments in multi-energy conversion, storage, and demand-side management systems under uncertainty. IEEE Trans Sustain Energy 2011;2:194–202.
[56] Enefield, Fuel Cells, Combined Heat and Power. 〈http://enefield.eu/systems-information/〉; 2013.
[57] Escher W, Paredes S, Zimmermann S, Ong CL, Ruch P, Michel B. Thermal management and overall performance of a high concentration PV. In: Proceedings of the conference on photovoltaic systems: CPV8 1477; 2012. p. 239–43.
[58] Michel B, Paredes S. Combining photovoltaic and thermal systems for efficiency gains. 〈http://spie.org/x102789.xml〉; 2013.
[59] DLR, National Aeronautics and Space Research Centre of the Federal Republic of Germany. 〈http://www.dlr.de/dlr/en/desktopdefault.aspx/tabid-10081/151_read-5495//year-all/#gallery/7975〉; 2013.
[60] Khadir MT, Fay D, Boughrira A. Day type identification for algerian electricity load using Kohlen maps. Int J Appl Math Comput Sci 2004;1(2):112–6.
[61] Ministère de'Energie et des Mines. 〈http://www.mem-algeria.org/francais/index.php?page=potentiels-national-des-energies-renouvelables〉; 2013.
[62] IEA, Energy Technology Network, Solarpaces. 〈http://www.solarpaces.org/_Libary/START_Algeria_2003.pdf〉; 2013.
[63] Bader R, Steinfeld AA. Solar trough concentrator for pill-box flux distribution over a CPV panel. ASME J Sol Energy Eng 2009;132(1):145011–4(Techical brief).
[64] Ermer JH, Jones RK, Hebert P, Pien P, King RR, Bhusari D, et al. Status of C3MJ and C4MJ production concentrator solar cells at Spectrolab. IEEE J Photovolt 2012;2(2):209–13.
[65] Jones RK, King RR, Fetzer CM, Ermer JH, Edmondson KM, Hebert P. Analysis of energy production of Spectrolab multijunction solar cells in field conditions. In: Proceedings of the 38th IEEE photovoltaic specialists conference (PVSC); 2012. p. 2065–70.
[66] Escher W, Ghannam R, Khalil ASG, Paredes S, Michel B. Advanced liquid cooling of multi chip modules for concentrated photovoltaic electric and thermal power co-generation. In: Proceedings of the IEEE Xplore, Theta 3; 2010.
[67] Valero A, Lozano MA, Munoz M. A general theory of exergy saving I, II and III. New York, USA: ASME Books; 1986; 1–21.
[68] Art S. Minimizing exergetic losses in multi-carrier energy systems. Semester Paper, ETHZ; 2009. p. 1–33.
[69] Demir H, Mobedi M, Ülkü S. A review on adsorption heat pump: problems and solutions. Renew Sustain Energy Rev 2008;12:2381–403.
[70] Wang R, Ge T, Chen C, Ma Q, Xiong Z. Solar sorption cooling systems for residential applications: options and guidelines. Int J Refrig 2009;32:638–60.
[71] Núñez T, Mittelbach W, Henning HM. Development of an adsorption chiller and heat pump for domestic heating and air-conditioning applications. Appl Therm Eng 2007;27:2205–12.
[72] Gebhardt M, Kohl H, Steinrötter T. Preisatlas: Ableitung von Kostenfunktionen für Komponenten der rationellen Energienutzung. Institut für Energie und Umwelttechnik e.V. (IUTA); 2002 p. 1–356.
[73] Moran MJ, Shapiro HN. Fundamentals of engineering thermodynamics book. English. 6th ed. Hoboken: Wiley; 2008.
[74] Incropera FP, DeWitt DP, Bergmann TL, Lavine AS. Fundamentals of heat and mass transfer. 7th ed. Hoboken: Wiley; 2013.
[75] Lozano MA, Valero A, Serra L. Theory of exergetic cost and thermoeconomic optimization. Energy Syst Ecol 1993:339–50.
[76] Tsatsaronis G, Pisa J. Exergoeconomic evaluation and optimization of energy systems – the CGAM problem. Energy 1994;19(3):287–321.
[77] Erlach B, Serra L, Valero A. Structural theory as standard for thermoeconomics. Energy Convers Manag 1999;40(15–16):1627–49.
[78] Seyboth K, Beurskens L, Langniss O, Sims REH. Recognising the potential for renewable energy heating and cooling. Energy Policy 2008;36(7):2460–3.
[79] Filippini M, Alberini A. Response of residential electricity demand to price: the effect of measurement error. Energy Econ 2011;33(5):889–95.
[80] Comparative Study of Electricity Tariffs used in Africa, UPDEA. 〈http://www.updea-africa.org/updea/DocWord/TarifAng2010.pdf〉; 2010.
[81] IMF, Statistical Appendix. 〈http://www.imf.org/external/pubs/ft/weo/2011/02/pdf/statapp.pdf〉; 2011.
[82] Zimmermann S, Tiwari MK, Meijer I, Paredes S, Michel B, Poulikakos D. Hot water cooled electronics: exergy analysis and waste heat reuse feasibility. Int J Heat Mass Transf 2012;55:6391–9.
[83] Krugman P. The myth of Asia's miracle. Foreign Aff 1994;73(6):62–78.
[84] World Bank. Electricity Consumption in Algeria. 〈http://data.worldbank.org/country/algeria〉; 2012.
[85] Bernstein MA, Griffin J. Regional differences in the price elasticity of demand for energy. Technical Report 2005. RAND Corporation.
[86] CIA database. 〈https://www.cia.gov/library/publications/the-world-factbook/geos/ag.html〉; 2013.